

1      **Invariant Image Reparameterisation: A Unified Approach to Structural and**  
2      **Practical Identifiability and Model Reduction**

3      Oliver J. Maclaren\*, Ruanui Nicholson\*, Joel A. Trent\*, Joshua Rottenberry†, and  
4      Matthew J. Simpson‡

6      **Abstract.** Both structural and practical parameter non-identifiability present fundamental challenges when  
7      using mathematical models to interpret data. This issue is particularly acute in complex, applied  
8      areas such as the life sciences or engineering, where determining appropriate model complexity is chal-  
9      lenging. While several approaches exist for diagnosing and resolving parameter non-identifiability,  
10     including symbolic methods, profile likelihood analysis, and sloppiness analysis, these approaches  
11     have distinct limitations and are rarely combined. We present a novel integrated approach called  
12     Invariant Image Reparameterisation (IIR) that incorporates key elements of these methods in a new  
13     way. Our approach replaces symbolic computations with numerical calculations at a single reference  
14     estimate and an invariance condition that determines when this local calculation holds globally. Pa-  
15     rameter combinations determined by this method are naturally ordered by degree of identifiability,  
16     and this supports model reduction by replacing a practically non-identified model with a structurally  
17     non-identified approximate model. This approximate model can be further parameterised in terms of  
18     identified parameters only. By treating parameter combinations determined by our approach as in-  
19     terest parameters within our established likelihood-based Profile-Wise Analysis (PWA) framework,  
20     we incorporate uncertainty quantification in terms of likelihood profiles and confidence sets. We  
21     provide a Julia library on [GitHub](#) demonstrating our methodology across a range of mathematical  
22     models.

23      **Key words.** Identifiability, Parameter estimation, Model reduction, Uncertainty quantification, Prediction

24      **1. Introduction.** Mechanistic mathematical models are widely used for interpreting ex-  
25      perimental and observational data and learning about underlying causes of the observed  
26      phenomena. Such models are routinely used to provide insight into a broad range of ap-  
27      plications including engineering (e.g. material science [36], fluid dynamics and transport  
28      phenomena [4, 28, 62, 6, 39]), ecology and population biology [38], disease transmission dy-  
29      namics [56] as well as chemical reactions [35] and econometrics [32]. A fundamental challenge  
30      is determining whether available data contain enough information to yield unique or suffi-  
31      ciently precise parameter estimates, which are crucial both for understanding mechanisms  
32      and making predictions [64, 65].

33      Establishing whether model parameters are uniquely determined is often referred to as  
34      *structural identifiability analysis* in the modelling literature [5, 16, 45, 50, 51, 25], and is  
35      also simply referred to as identifiability analysis in the statistical literature [46]. In contrast,  
36      learning whether sufficiently precise parameter estimates are possible when working with fi-  
37      nite noisy observations corresponds to the notion of *practical identifiability* (or estimability)  
38      analysis [33, 46, 70, 41].

39      Parameter non-identifiability occurs when different combinations of parameters produce

---

\*Department of Engineering Science and Biomedical Engineering, University of Auckland, Auckland 1142, New Zealand.

†School of Mathematical Sciences, Queensland University of Technology (QUT), Brisbane, Australia.

‡ARC Centre of Excellence for the Mathematical Analysis of Cellular Systems, QUT, Brisbane, Australia.

40 identical, or sufficiently close, model outputs. making it impossible to uniquely determine the  
 41 underlying mechanisms from observations [46, 65].

42 When model parameters are not identifiable, key questions arise: Can we identify certain  
 43 parameter combinations even when individual parameters are non-identifiable [46, 17]? Can  
 44 we perform model reduction to obtain simpler, identifiable models [13, 14, 27, 50, 51, 17]? Can  
 45 we use practical non-identifiability to guide experimental design [63] or motivate approximate  
 46 model reduction [49]?

47 Existing approaches include symbolic methods [13, 14, 18, 15], profile likelihood analy-  
 48 sis [40, 60, 49, 64, 68], and sloppiness analysis [8, 31, 54]. Related work includes active sub-  
 49 spaces [19] and likelihood-informed dimension reduction [23, 24] for large-scale inverse prob-  
 50 lems. While each approach has strengths, they also have limitations: symbolic methods typi-  
 51 cally apply only to idealised data/structural identifiability scenarios, profile likelihood methods  
 52 usually require manual choice of target parameter to analyse, and sloppiness analysis may use  
 53 non-parameterisation-invariant approximations for uncertainty quantification. Furthermore,  
 54 the relationship between sloppiness and identifiability is not always clear, as sloppiness is a  
 55 relative notion quantified in terms of ratios of eigenvalues (or singular values) models can  
 56 be sloppy yet identifiable [16]. In applications of sloppiness and profile likelihood analysis to  
 57 model reduction, users often simply set poorly-identified parameters to zero or some arbitrary  
 58 value [42, 26, 69]. However, this can lead to setting individually poorly-identified parameters  
 59 to values that jointly violate the requirements on possible values for the well-identified param-  
 60 eter combinations. Model reduction methods for inverse problems [19, 23], while powerful for  
 61 computation, particularly Bayesian inverse problems, do not typically directly address iden-  
 62 tifiability questions and do not usually aim to provide interpretable parameter combinations  
 63 for mechanistic models.

64 We present a novel approach that: (i) automatically identifies well-identified parameter  
 65 combinations without symbolic computation; (ii) enables model reduction without requiring  
 66 an explicit reduced form model; and (iii) provides statistically sound interval estimates for  
 67 both parameters and predictions. Our method combines ideas from symbolic analysis and  
 68 sloppiness literature to convert the general symbolic problem to a numerical one solvable at  
 69 a single reference point. These parameter combinations then serve as interest parameters  
 70 in our Profile-Wise Analysis (PWA) framework [65, 64]. For certain parameter combination  
 71 classes, we recover structural identifiability analysis results to arbitrary accuracy, while still  
 72 discovering useful approximate combinations in other cases.

73 **2. Methods.** Here, we outline the technical foundations of our ‘Invariant Image Repa-  
 74 ramesterisation’ approach, which builds on and extends the frameworks reviewed in [18], [17],  
 75 [64], and, indirectly, [46, 47]. Our approach consists of four key components: (1) an auxiliary  
 76 mapping connecting model parameters to observable quantities, (2) a general reparameterisa-  
 77 tion framework, (3) an initial parameter transformation to enable numerical computation, and  
 78 (4) a singular value decomposition for implementing the reparameterisation in transformed  
 79 parameter space. The identified parameter combinations can then serve as interest parame-  
 80 ters in our Profile-Wise Analysis (PWA) workflow [64] or alternative approaches like Bayesian  
 81 inference, which can also benefit from reparameterisation methods [29].

**2.1. Terminology.** We work relatively informally with (assumed-to-be) smooth mappings between finite-dimensional spaces [44], using standard terminology for submersions – mappings with full rank derivative – and immersions – mappings with injective derivative. The observed Fisher information measures parameter information content via the negative Hessian of the log-likelihood [58, 20, 59]. Informally, parameters or parameter combinations are identifiable if they can be uniquely determined from ‘perfect data’. In the context of a model mapping parameters to data distributions,  $\theta \mapsto p(y; \theta)$ , this is equivalent to the mapping, or more generally an induced relation in terms of parameter combinations, being injective [46].

**2.2. Model representation.** The auxiliary mapping  $\phi$  connects model parameters to data distribution parameters [64]:

$$\theta \mapsto \phi(\theta),$$

with density function

$$p(y; \phi),$$

inducing the probability model

$$p(y; \theta) = p(y; \phi(\theta)).$$

For spatial/temporal models, we use numerical solutions on a fine grid as the ‘exhaustive’ summary, evaluating derivatives via automatic differentiation in Julia [61]. Thus, while our approach is essentially identical to the ‘exhaustive summary’ approach reviewed by [18, 17], we generally avoid the need for explicit exhaustive summary methods such as Taylor series or generating series (as reviewed in the cited articles), though these can be used if available. In this context, we emphasise that automatic differentiation at the source code level is distinct from symbolic differentiation and only evaluates the numerical value of the derivative at a fixed input value [30].

The observed Fisher information in  $\theta$  coordinates is:

$$(2.4) \quad \mathcal{J}(\theta) = -H_l(\theta; y) = -\nabla_\theta(D_\theta l(\theta; y))^T = -\frac{\partial^2 l(\theta; y)}{\partial \theta \partial \theta^T}$$

where  $l(\theta; y)$  is the log-likelihood,  $D_\theta f$  is the Jacobian,  $\nabla_\theta f$  is the gradient, and  $H_f$  is the Hessian [48].

**2.3. Decomposition of the auxiliary mapping.** The auxiliary mapping can be decomposed as:

$$(2.5) \quad \phi(\theta) = \tilde{\phi}(\psi(\theta)),$$

where  $\psi(\theta)$  represents identifiable parameter combinations and  $\tilde{\phi}$  provides a one-to-one mapping to data distribution parameters. This decomposition is guaranteed by the epi-mono factorisation property of the general category of sets and mappings [43], where any mapping  $f : A \rightarrow B$  between sets  $A$  and  $B$  factorises as the composition:

$$(2.6) \quad f = m \circ e,$$

117 where  $e : A \rightarrow C$  is onto (epimorphic),  $m : C \rightarrow B$  is one-to-one (monomorphic), and  $C$  is  
 118 some intermediate space, called the *image*,  $\text{im}(f)$ , in the context of category theory. Conceptually,  
 119 this represents the possibility of a reduced model taking just the identified parameter  
 120 combinations. Here we aim to determine this intermediate image by a local calculation that  
 121 is ‘invariant’ to the choice of calculation point.

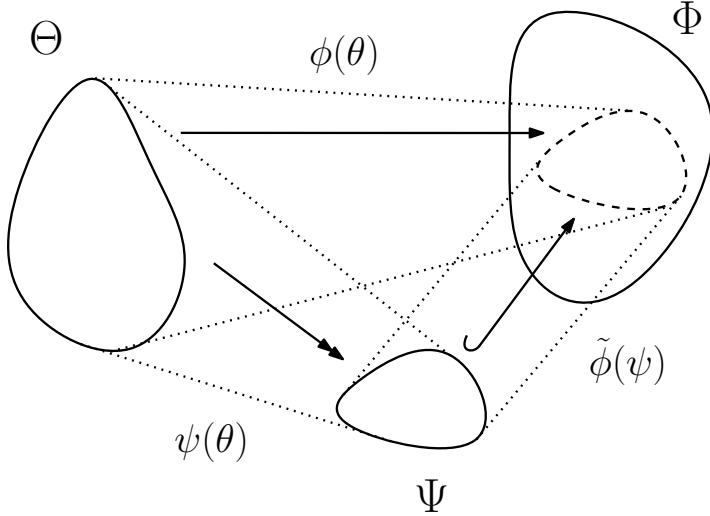


Figure 1: The basic decomposition of the auxiliary mapping into an identifiable reparameterisation followed by a reduced model mapping. Here  $\theta$  represent the original model parameters,  $\psi(\theta)$  represents identifiable parameter combinations, and  $\tilde{\phi}$  provides a one-to-one mapping from identifiable parameter combinations to data distribution parameters.

122 **2.4. Symbolic reparameterisation condition.** For smooth mappings with constant rank,  
 123 we can strengthen the epi-mono factorisation by requiring  $\psi(\theta)$  to be a smooth submersion  
 124 and  $\tilde{\phi}(\psi)$  to be a smooth immersion [44]. The chain rule then gives:

125 (2.7) 
$$D_\theta \phi(\theta) = D_\psi \tilde{\phi}(\psi(\theta)) D_\theta \psi(\theta).$$

126 Since  $D_\psi \tilde{\phi}(\psi(\theta))$  is one-to-one, the rank of  $D_\psi \tilde{\phi}(\psi(\theta))$  and  $D_\theta \phi(\theta)$  are the same; furthermore,  
 127 these derivatives share the same null space/kernel (see supplementary material):

128 (2.8) 
$$\ker D_\theta \psi(\theta) = \ker D_\theta \phi(\theta).$$

129 Given null space vectors  $\alpha(\theta)$  obtained from  $D_\theta \phi(\theta)$ , we can then solve:

130 (2.9) 
$$D_\theta \psi(\theta) \alpha(\theta) = 0,$$

131 for  $\psi(\theta)$ . This is equivalent to the conditions given by e.g. [12, 13], summarised by [18, 17].  
 132 It’s also equivalent to equating the rows of  $D_\theta \psi(\theta)$  to the vectors spanning the row space of  
 133  $D_\theta \phi(\theta)$ . The image of these vectors under  $\psi$  gives the intermediate ‘image’ component  $C$  of

134 the epi-mono factorisation. As shown in detail in the supplementary material, we can also  
 135 work directly with the observed Fisher information by solving a null space constraint in terms  
 136 of the Fisher information rather than the Jacobian derivative of the auxiliary mapping. If  
 137 we use the limiting, i.e. infinite data, Fisher information, these approaches are equivalent,  
 138 otherwise additional finite data effects are included in the Fisher information formulation (see  
 139 below).

140 **2.5. Parameter space linearisation.** Our goal is to determine identifiable parameter  
 141 combinations without symbolic computation. While numerical methods typically provide  
 142 only local reparameterisation information, we show that an initial coordinate transforma-  
 143 tion enables global results. Here we focus on the componentwise log transformation  $\log \theta =$   
 144  $[\log \theta_1, \log \theta_2, \dots, \log \theta_p]^T$ , which linearises monomial parameter combinations in parameter  
 145 space, though the overall function will still typically be a nonlinear function of the resulting  
 146 linear combinations of log parameters. Reduced sets of monomial parameter combinations  
 147 commonly arise in mechanistic models, e.g. via the Buckingham Pi theorem of dimensional  
 148 analysis [10], and related asymptotic approximations and model reduction [3]. Such a log  
 149 parameter transformation is commonly used in the sloppiness literature [7, 53, 69] and this  
 150 also inspired our present approach. However, our basic approach can be applied if, e.g., only  
 151 some components are logged or even if both logged and unlogged parameters are considered  
 152 simultaneously.

153 Working in log coordinates, defining  $\theta^* = \log(\theta)$  to be the component-wise log of the  
 154 parameter vector, models with monomial parameter combinations take the form:

155 (2.10) 
$$\phi(\theta) = \tilde{\phi}(\exp(A\theta^*)),$$

156 where  $A$  is a matrix of real coefficients. The chain rule gives:

157 (2.11) 
$$D_{\theta^*}\phi_*(\theta^*) = D_{\psi_*}\tilde{\phi}(\psi_*(\theta^*))\text{diag}(\exp(A\theta^*))A,$$

158 leading to our key condition:

159 (2.12) 
$$\ker A = \ker D_{\theta^*}\phi_*(\theta^*).$$

160 This follows since (see supplementary material), the first two terms in the right-hand side of  
 161 the chain rule equation, (2.11), compose to give an injective mapping and leave the null space  
 162 unchanged. As the left-hand side of (2.12) is parameter-independent, the right-hand side  
 163 must be too. We can hence evaluate the right-hand side derivative at any convenient point to  
 164 determine the global, invariant null space, complementary row space and hence intermediate  
 165 image, reducing what would be a PDE to an algebraic computation. If the model is assumed  
 166 non-identifiable, the point used will generally be, e.g., any (non-unique) maximum likelihood  
 167 estimate, and the Jacobian will be singular. This is expected and causes no issues in general.

168 While this condition does not uniquely determine  $A$ , as any basis for the null space (and  
 169 complementary row space) can be used, it establishes the existence of a matrix capturing  
 170 non-identifiable and identifiable parameter combinations. While the coefficients in  $A$  are tra-  
 171 ditionally restricted to integers in dimensional analysis, here we allow them to be arbitrary

real numbers and do not require the combinations to be dimensionless *a priori*. This relaxation facilitates numerical computation and provides more flexibility in discovering practically useful parameter combinations. However, we also consider *a posteriori* scaling and rounding operations to convert these real-valued coefficients to integers to aid interpretability while preserving key properties of the approximation.

The corresponding alternative route to the decomposition of the auxiliary mapping is illustrated in Figure 2.

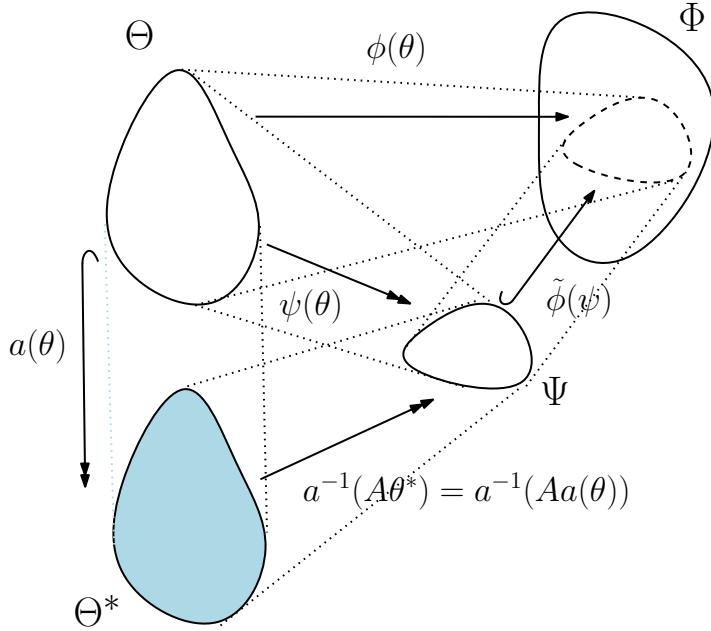


Figure 2: Implementation of parameter space linearisation using an initial componentwise transformation  $a(\theta)$ , typically log, followed by a linear transformation and componentwise inverse. The chain rule applied on the path from  $\Theta^*$  to  $\Phi$  allows us to equate the overall null space to that of the constant linear transformation  $A$ .

**2.6. Singular value decomposition for nonlinear parameter combinations.** Given the Jacobian in log-parameters at reference point  $\hat{\theta}^*$ , we compute:

$$(2.13) \quad D_{\theta^*}\phi_*(\hat{\theta}^*) = U\Sigma V^T = U_r\Sigma_r V_r^T$$

Taking  $A = V_r^T$ , or any row-scaled version of this, ensures the same kernel as  $D_{\theta^*}\phi_*(\hat{\theta}^*)$ . The singular values provide a natural ranking of parameter combinations by identifiability, with zero or near-zero values indicating structural or practical non-identifiability respectively.

We can also partition parameters into identifiable and non-identifiable combinations using the full rather than reduced SVD:

$$(2.14) \quad \theta \mapsto \begin{bmatrix} \psi(\theta) \\ \lambda(\theta) \end{bmatrix} = \exp(V^T \log(\theta))$$

188 where  $\psi(\theta)$  corresponds to non-zero singular values and associated singular vectors, and  $\lambda(\theta)$  to  
 189 (near) zero values and associated singular vectors. This maintains compatibility with existing  
 190 model codes while capturing the identifiability structure.

191 In the case of practical non-identifiability, or near non-identifiability, there will be singular  
 192 values close to zero, and the corresponding singular vectors will be elements of the row space  
 193 rather than the null space of the Jacobian. As the SVD leads to an orthogonal basis these  
 194 singular vectors can still be considered to span a self-contained ‘practically non-identifiable’  
 195 parameter space (see e.g. [66]), and the remaining singular vectors will still span the well-  
 196 identified parameter space.

197 As mentioned above, the null space and row space of the limiting observed Fisher information  
 198 are the same as that of the auxiliary mapping, we can also extend this approach to  
 199 work directly with the observed Fisher information (supplementary information). This may  
 200 be more natural for many models.

201 **2.7. Practical vs structural identifiability and observation operators.** An important  
 202 aspect of the relationship between practical and structural identifiability is represented by the  
 203 need for observation operators such as:

204 (2.15) 
$$\phi_{\text{obs}} = B_{\text{obs}} \phi_{\text{fine}}$$

205 where  $B_{\text{obs}}$  maps the fine-scale (numerical) solution to (experimental) observation points.  
 206 The additional loss of information due to coarser observation scale can introduce additional  
 207 null space components or poorly-identified parameters depending on the degree of additional  
 208 discretisation. When we discuss the limiting observed Fisher information, we mean the ob-  
 209 served Fisher information at the solution grid level; this is required for the Fisher information  
 210 analysis to match the structural identifiability analysis, otherwise additional null space/poorly-  
 211 identified components may be introduced.

212 When analysing at the solution grid level, our results should, to numerical approximation,  
 213 recover those from an idealised structural identifiability analysis. However, for ill-posed prob-  
 214 lems or models with parameter-dependent limiting behavior, the distinction between practical  
 215 and structural non-identifiability can blur [46]. The auxiliary mapping may have arbitrarily  
 216 small singular values in certain parameter regions, making the distinction between practical  
 217 and structural non-identifiability less clear. Furthermore, it is unclear if ideal structural iden-  
 218 tifiability results are useful in the absence of practical identifiability [46]. Our approach here  
 219 is to use the auxiliary mapping (or limiting Fisher information) to determine the reparam-  
 220 eterisation, but carry out the likelihood-based uncertainty analysis at the observation grid  
 221 level. This provides a practical identifiability analysis that is consistent with the structural  
 222 identifiability analysis

223 **2.8. Scaling and rounding.** For numerical implementation, we apply scaling and rounding  
 224 to singular vectors to obtain interpretable parameter combinations, defaulting to the nearest  
 225 0.5 when scaling relative to the smallest non-zero singular value. The continuity of singular  
 226 subspaces [66] ensures stable separation of parameter combinations in cases of near non-  
 227 identifiability, with practically (non-)identifiable subspaces corresponding to structurally (non-  
 228 )identifiable subspaces of the limit model.

**2.9. Profile-wise analysis.** We quantify uncertainty using our PWA framework [64], which connects identifiability, parameter estimation, and predictive uncertainty through likelihood-based confidence sets. This approach uses both the joint likelihood for all parameters and profiles of the likelihood – the likelihood as a function of a target parameter with the other ‘nuisance’ parameters maximised out [40, 60, 20, 59]. As the likelihood function is invariant to reparameterisation [58, 59, 20], reparameterisation of the full likelihood preserves all information in the original likelihood, unlike quadratic approximations based on the Fisher information. Rather, reparameterisation presents the information in the likelihood in a clearer form, while profile likelihoods reveal identifiability of individual parameters, or parameter combinations, separately from nuisance parameters [2].

**3. Example models.** Here, we describe three examples of varying areas of application and complexity, covering statistics and data science (parameterised normal distributions based on approximations to the binomial and Poisson models) [57, 2, 1], biochemistry and bioengineering (Michaelis-Menten kinetics) [52, 37], and physics and engineering (groundwater flow, heat conduction, diffusive and other transport modelling) [4, 28, 62, 11, 22, 6].

**3.1. Parameterised normal approximations.** Our first example considers estimating the number of trials  $n$  and success probability  $p$  in a continuous approximation to a binomial model. Near the Poisson limit (large  $n$ , small  $p$ ), maximum likelihood estimates become unstable [57], providing a case study in practical non-identifiability.

248 The model for a single (' $n$ -trial') experiment is:

$$249 \quad (3.1) \qquad \qquad \qquad Y \sim \mathcal{N}(np, np(1 - np)),$$

250 with Poisson limit case:

$$251 \quad (3.2) \qquad \qquad \qquad Y \sim \mathcal{N}(np, np).$$

252 The auxiliary mapping connects the underlying  $(n, p)$  ‘mechanistic’ parameters to normal  
253 distribution parameters:

$$254 \quad (3.3) \qquad \phi : \begin{bmatrix} n \\ p \end{bmatrix} \mapsto \begin{bmatrix} np \\ np(1-p) \end{bmatrix} = \begin{bmatrix} \mu \\ \sigma^2 \end{bmatrix}.$$

255 Although this is not really a ‘mechanistic’ model in the usual sense, one could consider an  
 256 underlying binomial model as a lower-level mechanism that ‘generates’ the higher-level (ap-  
 257 proximately) normally distributed observations. The problem is to determine both  $n$  and  $p$   
 258 given  $k$  observations from the single experiment model given by (3.1) or (3.2).

**3.2. Michaelis-Menten kinetics.** Our second example is the Michaelis-Menten model [37, 52]. This equation describes substrate depletion:

$$261 \quad (3.4) \qquad \qquad \qquad \frac{dS}{dt} = -\frac{\nu S}{K + S},$$

where  $S$  is substrate concentration,  $\nu$  is maximum growth rate, and  $K$  is the half-saturation constant. For low substrate concentrations relative to  $K$ , this model has practical identifiability issues (see [34] in the context of microbial growth models), and the model approximately

265 reduces to:

266 (3.5) 
$$\frac{dS}{dt} = -\frac{\nu}{K} S.$$

267 The auxiliary mapping takes parameter vector  $\theta = [\nu, K]^T$  to a vector of solution values  $s(\theta)$   
 268 defined on a fine time grid. For simplicity, we assume a normal distribution error model  
 269 with constant standard deviation  $\sigma = 0.05$ , though, e.g., log-normal errors or other error  
 270 models can also be considered easily within our framework [55] (see also the next example).  
 271 Observations then follow:

272 (3.6) 
$$s_{\text{obs}} \sim \mathcal{N}(B_{\text{obs}} s(\theta), \sigma^2 I),$$

273 where  $B_{\text{obs}}$  maps to observation points and  $\sigma = 0.05$ .

274 In our present work we use the (structural) auxiliary mapping to determine the repara-  
 275 terisation, but the point estimate is determined by using the likelihood based on the observed  
 276 data distribution above.

277 **3.3. Flow in composite media.** Our final example models groundwater flow in a hetero-  
 278 geneous aquifer [4, 28, 62], governed by:

279 (3.7) 
$$T_i \frac{d^2 h}{dx^2} + R = 0,$$

280 for regions  $i = 1, 2$ , with transmissivity  $T_i$  and recharge rate  $R$ . Boundary conditions enforce  
 281 zero head at endpoints and continuity at the interface:

282 (3.8) 
$$\begin{aligned} h_1(0) &= 0 \\ h_2(L) &= 0 \\ h_1(L/2) &= h_2(L/2) \\ -T_1 \frac{dh_1}{dx}(L/2) &= -T_2 \frac{dh_2}{dx}(L/2). \end{aligned}$$

283 Analogous models appear in heat conduction, diffusive transport, and other transport phe-  
 284 nomena [11, 22, 6].

285 The solution (supplementary information) depends only on ratios  $R/T_1$  and  $R/T_2$ , indi-  
 286 cating structural non-identifiability. Here we use a log-normal error model for the hydraulic  
 287 head values with constant standard deviation  $\sigma$ . Observations then follow:

288 (3.9) 
$$\log h_{\text{obs}} \sim \mathcal{N}(\log B_{\text{obs}} h(\theta), \sigma^2 I),$$

289 where  $\theta = [T_1, T_2, R]^T$ , and  $h(\theta)$  is the fine-scale solution.

290 **4. Results and Discussion.** Here we present the results of our analysis of the three ex-  
 291 ample models described in Section 3. The first example is simple but illustrates many of  
 292 the key conceptual components of our approach, including both structural and practical non-  
 293 identifiability; the second involves a differential equation in time that is solved numerically and  
 294 utilises automatic differentiation to compute the Jacobian of the auxiliary mapping; and the  
 295 third involves a differential equation in space that can be solved analytically but involves three  
 296 parameters and structural non-identifiability. For this last example, we show how parameter  
 297 non-identifiability and predictive uncertainty are related using the PWA approach.

298     **4.1. Parameterised Normal Models.** These examples are sufficiently simple that we can  
 299 illustrate the core ideas analytically, and so we first outline some analytical results, with  
 300 additional details in the supplementary material. We then present numerical results, produced  
 301 without assuming these analytical results were available, using generic model-agnostic code.

302     We focus our analytical illustration on the Poisson limit model for simplicity, defined  
 303 by (3.2). In this model, we expect only  $np$  to be identifiable, as the variance is equal to the  
 304 mean. We will show that both symbolic (original parameters) and numerical (log-transformed  
 305 parameters) approaches obtain this result.

306     We also present the results of numerical, likelihood-based analysis of both parameterised  
 307 normal models. We consider the likelihood functions in both original parameterisation and our  
 308 reparameterisations. Although the likelihood is invariant to reparameterisation, we see how  
 309 the reparameterisation ‘brings out’ the separation of information concerning the identifiable  
 310 and non-identifiable parameters.

311     **4.1.1. Analytical results: Poisson limit model, original parameterisation.** To first obtain  
 312 the symbolic result we note, as above, that the auxiliary mapping in terms of untransformed  
 313 parameters is given by

$$314 \quad \phi(n, p) = \phi\left(\begin{bmatrix} n \\ p \end{bmatrix}\right) = \begin{bmatrix} np \\ np \end{bmatrix}.$$

315     The Jacobian of this mapping is given by

$$316 \quad (4.1) \quad D\phi(n, p) = \begin{bmatrix} p & n \\ p & n \end{bmatrix}.$$

317     This is a function of  $n$  and  $p$  and clearly has a non-trivial null space for all  $n$  and  $p$ . As the  
 318 Jacobian and the associated null space depend on (are given as a function of)  $n$  and  $p$  we  
 319 refer to this as the ‘symbolic’ null space of the model. We can determine this by inspection,  
 320 noting that vectors of the form

$$321 \quad (4.2) \quad \alpha(n, p) = \begin{bmatrix} n \\ -p \end{bmatrix}$$

322     satisfy  $D\phi(n, p)\alpha(n, p) = 0$  for all  $n$  and  $p$ . Thus the symbolic null space has dimension one and  
 323 is spanned by the vector  $\alpha(n, p)$ ; furthermore, the row space of  $D\phi(n, p)$  hence has dimension  
 324 one and is spanned by a symbolic vector orthogonal to  $\alpha(n, p)$ . This implies that  $\psi(n, p)$  is  
 325 scalar-valued and can be determined by equating the (unknown) single row of  $D\psi(n, p)$  to  
 326 the (transpose of the) vector spanning the (known) row space of  $D\phi(n, p)$ . By inspection, we  
 327 see that the row space of  $D\phi(n, p)$  is spanned by the vector  $[p, n]^T$ , which is orthogonal to  
 328  $\alpha(n, p) = [n, -p]^T$ .

329     Thus we can determine  $\psi(n, p)$  equating the rows of  $D\psi(n, p)$  to the vectors spanning the  
 330 row space of  $D\phi(n, p)$ , or by solving the partial differential equation

$$331 \quad (4.3) \quad \frac{\partial\psi}{\partial n}n + \frac{\partial\psi}{\partial p}(-p) = 0,$$

332 based on the orthogonality of the rows of  $D\psi(n, p)$  and the vectors spanning the null space  
 333 of  $D\phi(n, p)$ . By inspection, we see that  $\psi(n, p) = np$  is a solution to these equations, and  
 334 hence the identifiable parameterisation is given by  $\psi(n, p) = np$ , as expected. This approach  
 335 is equivalent to that of [13, 27, 18, 17] but, as with their approach, requires symbolic deter-  
 336 mination of the Jacobian and the solution of partial differential equations. We now show how  
 337 our numerical approach can determine the same result without symbolic manipulation.

338 **4.1.2. Analytical results: Poisson limit model, log-transformed parameterisation.** We  
 339 now consider the Poisson limit model in log-transformed parameters. By definition (specif-  
 340 ically, from parameterisation invariance) the auxiliary mapping in terms of log-transformed  
 341 parameters satisfies

$$342 \quad (4.4) \quad \phi_*(n^*, p^*) = \phi_* \left( \begin{bmatrix} n^* \\ p^* \end{bmatrix} \right) = \phi \left( \begin{bmatrix} n \\ p \end{bmatrix} \right) = \phi \left( \exp \left( \begin{bmatrix} n^* \\ p^* \end{bmatrix} \right) \right),$$

343 where  $n^* = \log n$  and  $p^* = \log p$  and where  $\exp$  is the componentwise exponential function.  
 344 The right-hand side of the above equation is obtained from the definition of the auxiliary  
 345 mapping in terms of untransformed parameters:

$$346 \quad (4.5) \quad \phi \left( \begin{bmatrix} n \\ p \end{bmatrix} \right) = \begin{bmatrix} np \\ np \end{bmatrix} = \begin{bmatrix} \exp(n^*) \exp(p^*) \\ \exp(n^*) \exp(p^*) \end{bmatrix} = \begin{bmatrix} \exp(n^* + p^*) \\ \exp(n^* + p^*) \end{bmatrix}.$$

347 Thus the Jacobian of the auxiliary mapping in terms of log-transformed parameters is given  
 348 by

$$349 \quad (4.6) \quad D\phi_*(n^*, p^*) = \begin{bmatrix} \exp(n^* + p^*) & \exp(n^* + p^*) \\ \exp(n^* + p^*) & \exp(n^* + p^*) \end{bmatrix} = \exp(n^* + p^*) \begin{bmatrix} 1 & 1 \\ 1 & 1 \end{bmatrix}.$$

350 As expected, this takes the SVD form (up to normalisation of the singular vectors):

$$351 \quad (4.7) \quad D\phi_*(n^*, p^*) = \underbrace{\begin{bmatrix} 1 \\ 1 \end{bmatrix}}_{D_{\psi_*} \tilde{\phi}(\psi_*(\theta^*))} \underbrace{\exp(n^* + p^*)}_{\text{diag}(\exp(A\theta^*))} \underbrace{\begin{bmatrix} 1 & 1 \end{bmatrix}}_A,$$

352 where  $\theta^* = [n^*, p^*]^T$ ,  $A$  is the matrix of the constant linear transformation component of the  
 353 reparameterisation and  $D_{\psi_*} \tilde{\phi}(\psi_*(\theta^*))$  is the Jacobian of the auxiliary mapping in terms of  
 354 the transformed, identifiable parameters. The diagonal ‘matrix’ is a scalar in this case as the  
 355 intermediate image is represented by a single parameter. Since  $\psi_*(n^*, p^*) = \exp(n^* + p^*)$ , and  
 356 the output of the auxiliary mapping is

$$357 \quad (4.8) \quad \phi_*(n^*, p^*) = \begin{bmatrix} \exp(n^* + p^*) \\ \exp(n^* + p^*) \end{bmatrix} = \begin{bmatrix} \psi_*(n^*, p^*) \\ \psi_*(n^*, p^*) \end{bmatrix},$$

358 we have that  $D_{\psi_*} \tilde{\phi}(\psi_*(\theta^*))$  is also constant in this case. In more general classes of models,  
 359 the  $A$  matrix will remain constant, but the Jacobian of the auxiliary mapping in terms of the  
 360 identifiable parameters will depend on the parameters.

361 Thus we conclude that the identifiable parameterisation is given by

362 (4.9)  $\psi_*(n^*, p^*) = \exp(A\theta^*) = \exp\left(\begin{bmatrix} 1 & 1 \end{bmatrix} \begin{bmatrix} n^* \\ p^* \end{bmatrix}\right) = \exp(n^* + p^*) = \exp(\log n + \log p) = np.$

363 This is the same result as obtained in the symbolic analysis above. However, as the  $A$  matrix  
 364 here is constant, and corresponds (up to normalisation) to the singular vector of the Jacobian  
 365 of the auxiliary mapping in log-transformed parameters, we can determine it with a single  
 366 numerical evaluation of the Jacobian. This is the key advantage of our numerical approach.

367 We can also determine the non-identifiable parameters by considering the full SVD of the  
 368 Jacobian (or by finding orthogonal vectors to the identifiable parameter combination). As  
 369 before, this implies that the non-identifiable parameter combination is given by

370 (4.10)  $\lambda_*(n^*, p^*) = \exp\left(\begin{bmatrix} 1 & -1 \end{bmatrix} \begin{bmatrix} n^* \\ p^* \end{bmatrix}\right) = \exp(n^* - p^*) = \frac{n}{p}.$

371 **4.1.3. Numerical results: Poisson limit model.** Below we present the results of our  
 372 numerical analysis of the Poisson limit model. We show the likelihood functions in both the  
 373 original parameterisation and the ‘invariant image’ reparameterisation in Figure 3. We used  
 374 true parameter values of  $n = 100$  and  $p = 0.2$ , and a sample size of 10. We also imposed bounds  
 375 of  $[0, 500]$  and  $[0, 1]$  for  $n$  and  $p$ , respectively. For reproducibility, the data realisation used  
 376 was  $[21.9, 22.3, 12.8, 16.4, 16.4, 20.3, 16.2, 20.0, 19.7, 24.4]$ . This was generated from the *non-*  
 377 *limit* model, i.e. treating the limit model as an approximation at the analysis rather than data  
 378 generation stage. The analysis can be found in the [repository](#) at `examples/stat_model.jl`.

379 The top row of Figure 3 shows the likelihood in the original parameterisation,. We see a  
 380 long ‘banana’ shaped likelihood contour in the  $(n, p)$  plane, illustrating the existence of (ap-  
 381 proximately) equivalent parameter combinations lying along a curved relationship. The profile  
 382 likelihoods for each parameter illustrate the individual non-identifiability of the parameters.  
 383 The likelihood is completely flat for both parameters, other than where the bounds of the  
 384 parameter space are reached. Together these results imply that the two parameters are not  
 385 individually identifiable in this model, though there may be some combination of parameters  
 386 that is identifiable (i.e.  $np$ , as we have shown analytically).

387 The bottom row of Figure 3 shows the likelihood in reparameterised space. We see the like-  
 388 lihood is constant in the vertical,  $\frac{n}{p}$ , direction and varies only in the horizontal,  $np$ , direction.  
 389 This reflects the identifiability of the parameter combination  $np$ , and the non-identifiability of  
 390 the parameter combination  $n/p$ . Furthermore, this structure means the information concern-  
 391 ing the identifiable and non-identifiable parameters is completely separated, as the likelihood  
 392 factors into a product of a function of  $np$  and a (constant) function of  $n/p$  (see e.g. the dis-  
 393 cussion in [2, 21]). Thus we can, in principle, construct an autonomous reduced model based  
 394 on the identifiable parameter combination  $np$  (as can be seen analytically).

395 The profile likelihoods for the new parameters, shown in the bottom row of Figure 3  
 396 further illustrate the distinct identifiability properties of these parameter combinations. The  
 397 profile likelihood for  $np$  is a simple Gaussian-like function, showing good estimability, while  
 398 the profile likelihood for  $n/p$  is completely flat, demonstrating non-identifiability.

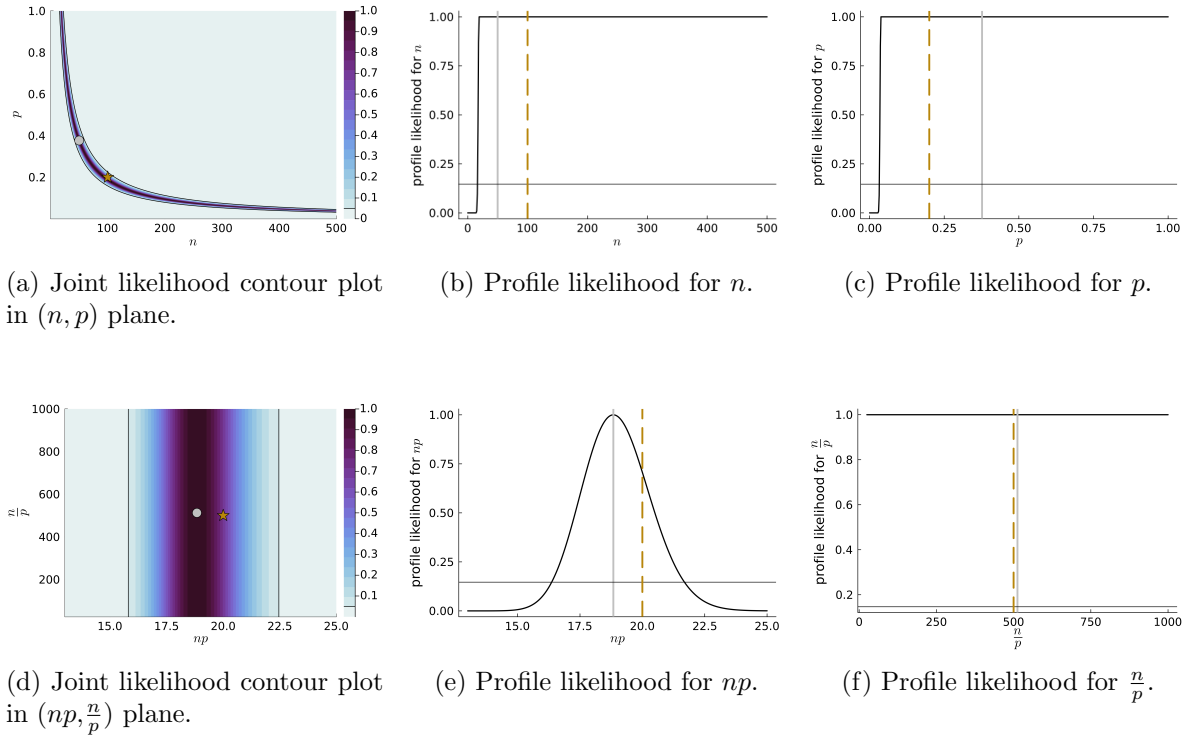


Figure 3: Poisson-limit example analysis in original (top row) and reparameterised (bottom row) parameter spaces. For the contour plots (left column), gold stars show the true parameter value, silver circles show the maximum likelihood estimate, and the colour bar represents the relative likelihood. For all plots, black contour/horizontal lines indicate the 95% confidence interval threshold. For profile likelihood plots (center, right columns), the solid silver vertical line indicates the maximum likelihood estimate, and the dashed gold vertical line indicates the true parameter value.

399     **4.1.4. Numerical results: non-limit model.** We now consider the non-limit model, de-  
 400     fined by (3.1). As can be verified analytically, this model is now technically identifiable  
 401     (supplementary material). However, near the Poisson limit, we also expect the parameters  
 402     to be practically non-identifiable, i.e. poorly-identified. In this setting, the well-identified pa-  
 403     rameter determined from the SVD will be close but not exactly equal to  $np$ , while there will  
 404     be a poorly identified parameter close to but not exactly equal to  $n/p$ . We can either work  
 405     with the exact SVD singular vectors obtained, e.g., for our point estimate, or use the heuris-  
 406     tic rounding approach to obtain the approximate reparameterisation. Here we find that our  
 407     rounding heuristic (dividing by smallest non-zero entry and rounding to nearest 0.5) indeed  
 408     recovers the previous identifiable and non-identifiable parameter combinations, but these now  
 409     correspond to ‘well-identified’ and ‘poorly but structurally identified’ parameters, respectively.  
 410     For these results, again, we used true parameter values of  $n = 100$  and  $p = 0.2$ , a sample  
 411     size of 10, and the same parameter bounds. For reproducibility, the data realisation used was

412 (again) [21.9, 22.3, 12.8, 16.4, 16.4, 20.3, 16.2, 20.0, 19.7, 24.4]. The analysis can again be  
 413 found in the [repository](#) at `examples/stat_model.jl`.

414 These results can be seen in Figure 4, and largely mirror those of the Poisson limit model.  
 415 The well-identified parameter  $np$  and the poorly identified parameter  $n/p$  are again clearly  
 416 separated in the reparameterised space. However, in this case, the separation is not exact,  
 417 and the poorly identified parameter is not completely flat in the profile likelihood. We also  
 418 see *one-sided identifiability* in both the original parameterisation and in the poorly identified  
 419 parameter in the reparameterised model – the likelihood is much flatter on one side of the  
 420 maximum likelihood estimate than the other. We can attribute this to the model becoming  
 421 poorly identified in the Poisson limit, which occurs asymmetrically in parameter space.

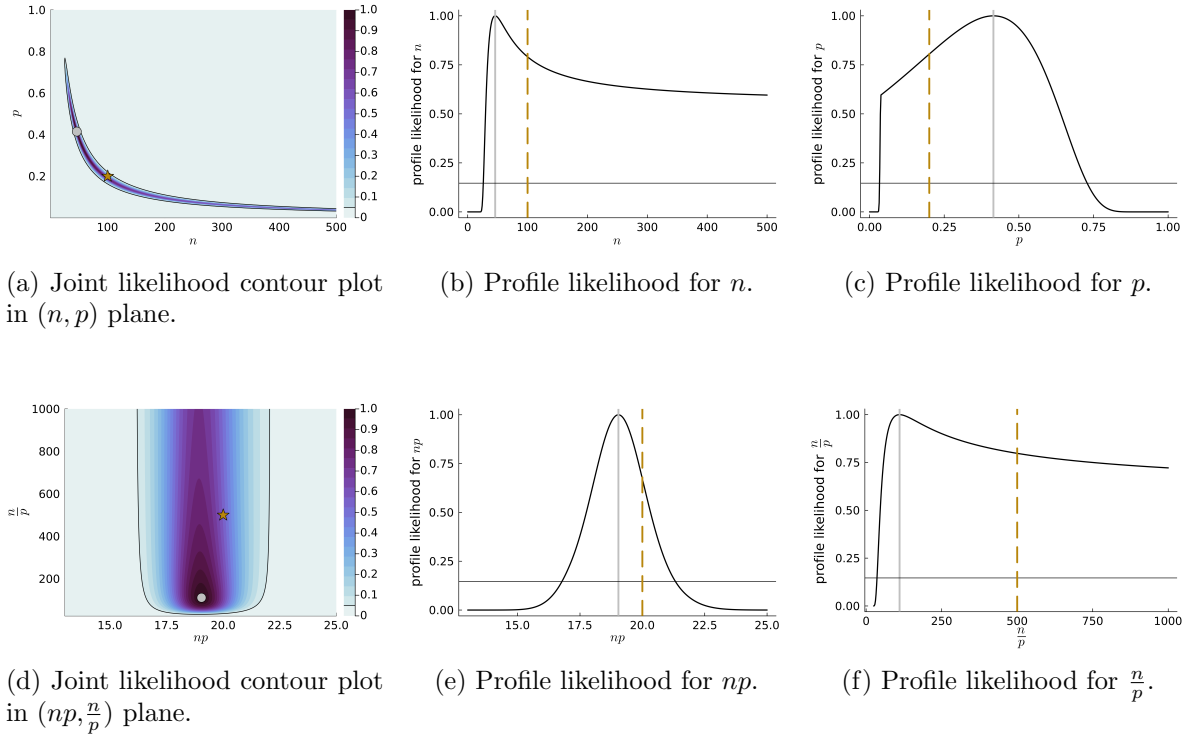


Figure 4: Non-limit (approximate Binomial) example analysis in original (top row) and reparameterised (bottom row) parameter spaces. For the contour plots (left column), gold stars show the true parameter value, silver circles show the maximum likelihood estimate, and the colour bar represents the relative likelihood. For all plots, black contour/horizontal lines indicate the 95% confidence interval threshold. For profile likelihood plots (center, right columns), the solid silver vertical line indicates the maximum likelihood estimate, and the dashed gold vertical line indicates the true parameter value.

422     **4.2. Michaelis-Menten kinetics.** We now consider the Michaelis-Menten kinetics model,  
 423 defined by (3.4). This model is structurally identifiable but practically non-identifiable in

424 the limit regime where the initial substrate concentration,  $S(0)$ , is low relative to the half-  
425 saturation constant,  $K$ . For this example, we focus on results from the non-reduced model  
426 and present the results of the limit model in the supplementary material.

427 For these results, we used an initial concentration of  $S(0) = 1$ , a true half-saturation  
428 constant of  $K = 5.0$ , and a maximum growth rate of  $\nu = 1.0$ . We used a normal observation  
429 model with standard deviation  $\sigma = 0.05$ , and observed the concentrations at 11 equally spaced  
430 time points between 0 and 20. We used a fine time grid of 201 points between 0 and 20 for  
431 the model solution in the auxiliary mapping computations. This regime is relatively close to  
432 the limit regime, but not so close that the effects are negligible. We expect the parameters  
433 to be potentially practically non-identifiable in this regime, but structurally identifiable. Our  
434 analysis can be found in the [repository](#) at `examples/mm_model.jl`.

435 The top row of Figure 5 shows the results of the non-reduced model analysis in the original  
436 parameterisation. We see that the joint likelihood contours in the  $(\nu, K)$  plane consist of  
437 ‘fanning’ lines, indicating the existence of parameter combinations having similar likelihood  
438 values. The profile likelihoods for each parameter show that the maximum likelihood estimate  
439 is close to the true parameter value in this particular case but that the likelihood is very flat  
440 to one side (excluding the effects of parameter bounds) and shows characteristic ‘one-sided  
441 identifiability’, i.e. limiting non-identifiability.

442 The bottom row of Figure 5 shows the results of the non-reduced model analysis in repa-  
443 rameterised space. Here the parameter combinations identified are  $\frac{K}{\nu}$  (well-identified) and  
444  $\nu K$  (poorly identified). The first parameter represents the time scale associated with the  
445 limit model. We see a similar likelihood contour shape to the previous model analysis, with  
446 an apparent limiting regime where the parameters are decoupled and one parameter is well-  
447 identified while the other is poorly identified. Outside of the limit regime, the relationship  
448 between the parameters is more complex, and the parameters are not as clearly separated.  
449 Since the likelihood is invariant to reparameterisation, analysis of the non-reduced model in  
450 any coordinate system is equally valid. The role of reparameterisation is to bring out the sep-  
451 aration of information concerning the potentially identifiable and non-identifiable parameters.

452 Although only approximate, these results do suggest a structurally non-identified reduced  
453 model may be useful, in the limit as  $K\nu$  becomes large while  $\frac{K}{\nu}$  stays constant. This cor-  
454 responds to the limit model mentioned in the model description section above. The supple-  
455 mentary material shows the results of the limit model analysis in reparameterised space. In  
456 the limiting case, the profile likelihoods show full non-identifiability of the poorly identified  
457 parameter and good identifiability of the well-identified parameter. For this model, we pro-  
458 vide prediction results using PWA in the supplementary material and provide more detailed  
459 prediction results for the transport model next.

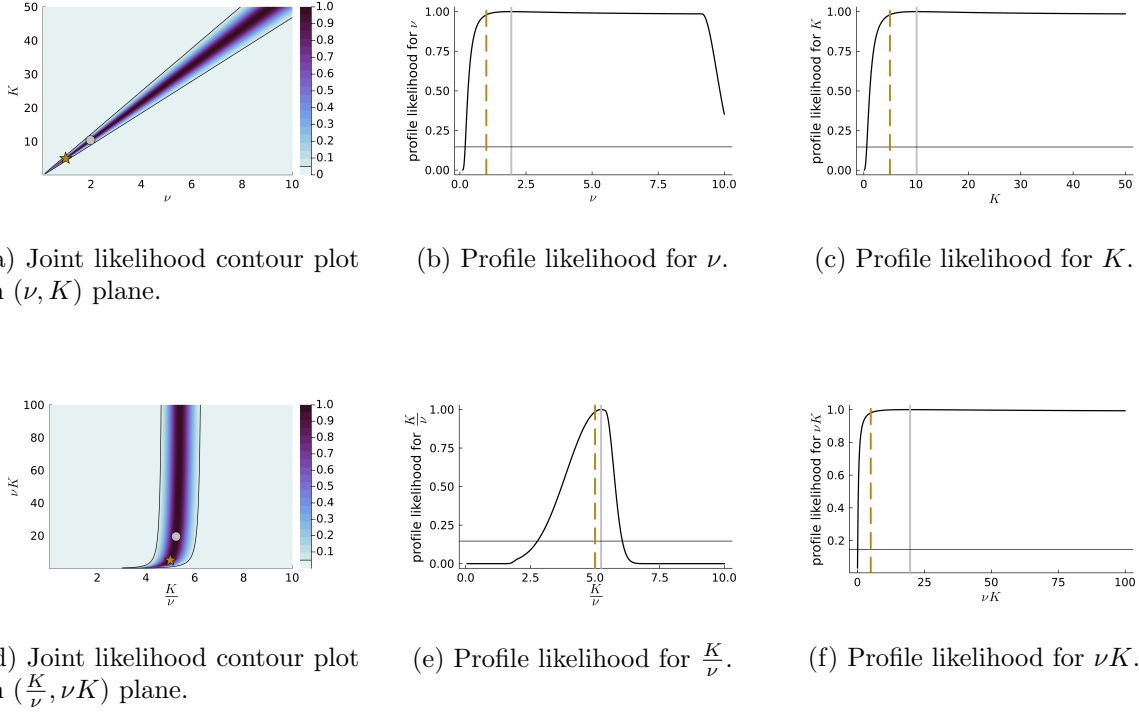


Figure 5: Michaelis-Menten example analysis in original (top row) and reparameterised (bottom row) parameter spaces. For the contour plots (left column), gold stars show the true parameter value, silver circles show the maximum likelihood estimate, and the colour bar represents the relative likelihood. For all plots, black contour/horizontal lines indicate the 95% confidence interval threshold. For profile likelihood plots (center, right columns), the solid silver vertical line indicates the maximum likelihood estimate, and the dashed gold vertical line indicates the true parameter value.

460     **4.3. Flow in composite media.** Here we consider the groundwater model, representing  
 461 flow in composite media, defined by (3.7). As discussed in the model section, and shown in  
 462 the supplementary material, this model is structurally non-identifiable, and can be written in  
 463 terms of a reduced set of monomial functions of the parameters. Rather than consider further  
 464 analytical results, we proceed directly to the numerical analysis of the model and verify that  
 465 our numerical approach can uncover the non-identifiability of the model and suggest a reduced  
 466 parameterisation.

467     For these results we used a true parameter value of  $T_1 = 3.0$ ,  $T_2 = 1.0$ , and  $R = 1.0$ , with  
 468 parameter bounds of  $[0.1, 5]$  for all quantities. We considered a fine grid of 201 points between  
 469  $x = 0$  and  $x = L = 100$ , and an observation grid of 19 equally-spaced points, excluding  
 470 the endpoints. We used a normal observation model with standard deviation  $\sigma = 0.2$  and  
 471 a single, spatial sample (i.e. a single observation of the model solution at the observation  
 472 points, giving a data vector of length 19). For reproducibility, the data realisation used was

473 [186.4, 402.6, 505.2, 756.1, 1144.1, 790.9, 1283.5, 1647.6, 872.3, 1144.4, 1691.2, 1352.7, 1519.9,  
 474 1316.0, 1437.1, 726.7, 952.3, 759.4, 272.0]. **repository** at `examples/transport_model.jl`.

475 The first two rows of Figure 6 show the results of the analysis in the original parameterisa-  
 476 tion. For visualisation we consider each of the three joint two-dimensional likelihood profiles  
 477 with the third parameter ‘profiled out’. We see that the joint profile likelihood contours in  
 478 the  $(T_1, T_2)$  plane show a ‘fanning out’ of the likelihood contours, indicating the existence of  
 479 parameter combinations having similar likelihood values. Similarly for  $(T_1, R)$ . For  $(T_2, R)$  we  
 480 see more concentrated contours, indicating that some combination of these parameters may  
 481 be better identified. We also show the one-dimensional profile likelihoods for each parameter.  
 482 These all show largely flat likelihoods, other than decreases induced by bounding constraints,  
 483 indicating that these parameters are not individually identifiable in this model.

484 The second two rows of Figure 6 show the analysis in the reparameterised space. The repa-  
 485 rameterisation suggested by the SVD is  $(\frac{T_2}{R}, \frac{T_1}{\sqrt{T_2}R}, T_1 T_2 R)$ , with the first having a singular  
 486 value two-three orders of magnitude larger than the second, and the third being numerically  
 487 equivalent to zero (order  $10^{-14}$ ). This indicates that one parameter combination is very well  
 488 identified, the second somewhat identified, and the third completely unidentifiable. The first  
 489 two combinations from the SVD reparameterisation are different to the reduced parameter  
 490 pair that appear in the analytical results, i.e. to  $(\frac{T_1}{R}, \frac{T_2}{R})$ , though these are in one-to-one  
 491 correspondence. This reflects that the SVD aims to find an orthogonal (in log-parameter  
 492 space in the present work) reparameterisation in which the information on each parameter  
 493 combination is maximally separated. Both pairs of parameter combinations are orthogonal to  
 494 the non-identified parameter combination  $T_1 T_2 R$  in log-space, and are linearly independent,  
 495 and hence provide a valid basis for the identified subspace. Here the two parameterisations  
 496 lead to visually indistinguishable results, and so we only show the results of the SVD repa-  
 497 rameterisation.

498 Notably, the reparameterised results indicate possible one-sided identifiability of the less  
 499 well (but still) identified parameter  $\frac{T_1}{\sqrt{T_2}R}$ , in addition to the structural non-identifiability of  
 500  $T_1 T_2 R$ . This suggests a further reduced limiting model may exist. Here the true value of  
 501 the first transmissivity parameter  $T_1$  is somewhat larger than the second (three vs one), and  
 502 the limit suggested by the one-sided non-identifiability is to take  $T_1$  large relative to  $T_2$  and  
 503  $R$ . Thus the smaller transmissivity parameter  $T_2$  becomes the limiting factor in the model,  
 504 and the model can be reduced to a simpler form. This reinforces that profile likelihood-based  
 505 practical identifiability methods can help determine limiting models [49].

506 Finally, we show the profile-wise prediction intervals for the full model in the repa-  
 507 rameterised space in Figure 7. We provide the profile-wise prediction intervals for the original  
 508 parameterisation in the supplementary material. We use a degree of freedom of two for all of  
 509 the prediction intervals (i.e. number of non-zero singular values; see also [67]). In the original  
 510 space the prediction intervals are driven by all three parameters (supplementary material). In  
 511 the reparameterised space, however, we see that the non-identified parameter  $T_1 T_2 R$  has no  
 512 effect on the prediction intervals. This is true of both the individual profile-wise prediction  
 513 interval based on  $T_1 T_2 R$  in the bottom row, and the joint prediction intervals involving  $T_1 T_2 R$   
 514 in the top row, which closely match the individual profile-wise prediction intervals for the  
 515 other parameter in each case.

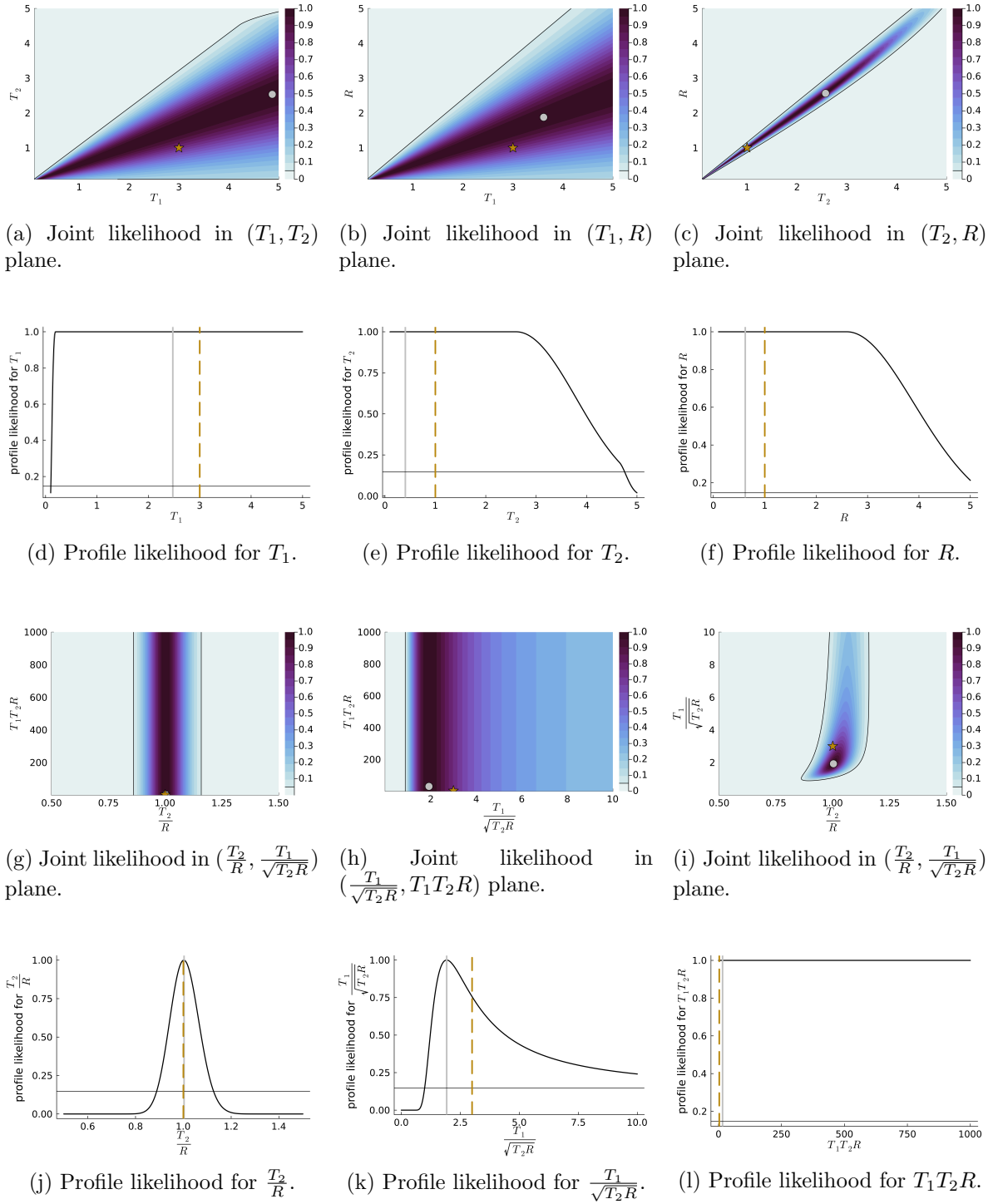


Figure 6: Flow in composite media example analysis in original (top two rows) and reparameterised (bottom two rows) parameter spaces. First and third rows show joint likelihood contours; second and fourth rows show profile likelihoods. For contour plots, gold stars show the true parameter value, silver circles show the maximum likelihood estimate, and colorbars represent relative likelihood. For all plots, black contour/horizontal lines indicate the 95% confidence interval threshold. For profile likelihood plots, solid silver vertical lines show maximum likelihood estimates and dashed gold vertical lines show true parameter values.

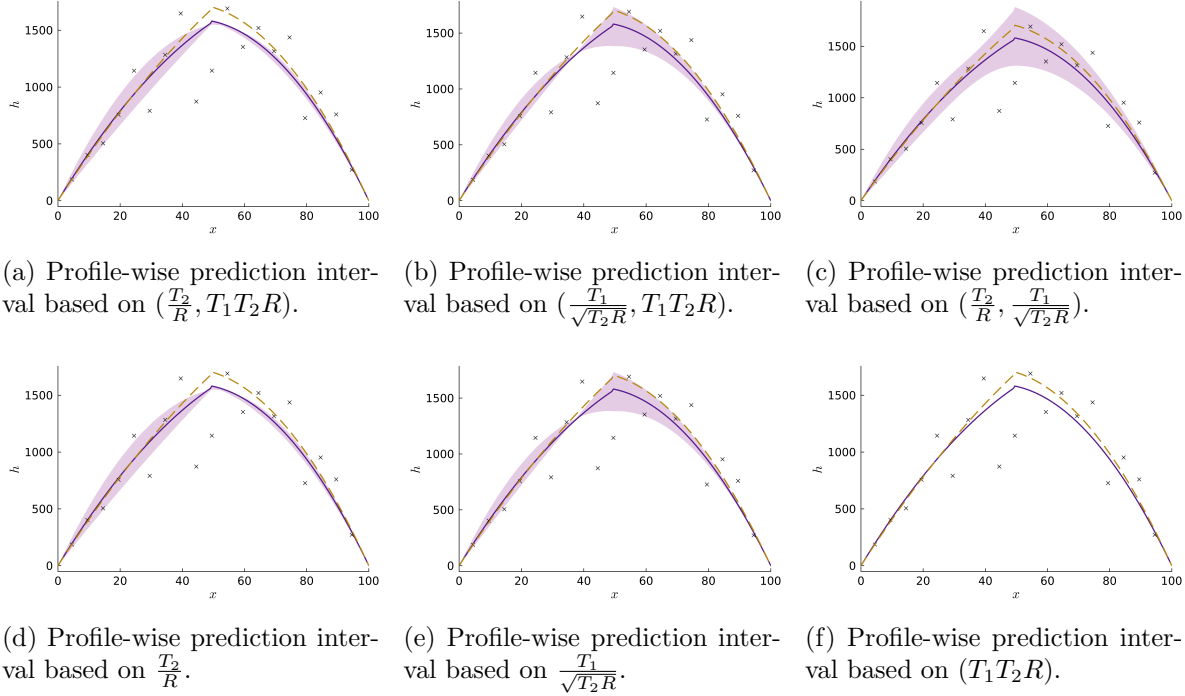


Figure 7: Profile-wise prediction intervals for the mean in the flow in composite media example in reparameterised space. Top row shows joint prediction intervals; bottom row shows individual parameter prediction intervals. In all plots, gold trajectories show the true mean function, dark purple trajectories show the maximum likelihood estimate, and purple shaded regions represent approximate 95% (predictive) confidence intervals for the mean.

516     **5. Conclusion and Future Work.** Here we have presented Invariant Image Reparameter-  
 517     isation (IIR), an approach to parameter identifiability analysis that bridges structural and  
 518     practical identifiability analysis, and symbolic and numerical approaches to implementation.  
 519     We show how an initial coordinate transformation converts the symbolic approach of discov-  
 520     ering identifiable parameter combinations into numerical computation at a single reference  
 521     point. This numerical approach recovers symbolic results for a common class of parame-  
 522     ter combinations while providing a natural ranking of such parameter combinations by their  
 523     degree of identifiability in general and in cases of practical non-identifiability.

524     We find that practical non-identifiability, particularly when one-sided or asymmetric, is  
 525     closely related to the existence of potential model reductions, mirroring observations by [49] on  
 526     using profile likelihood for model reduction. Our use of profile-likelihood-based Profile-Wise  
 527     Analysis for uncertainty quantification, in addition to Fisher information-based reparameteri-  
 528     sation, reveals such asymmetric limits in terms of likelihood contours and profiles, in contrast  
 529     to approaches focusing solely on Fisher-information/Hessian analysis.

530     As in [64], our approach extends to more complex models such as stochastic differential  
 531     equations or simulation-based models, given an appropriate auxiliary mapping. Here, we used

532 the full model solution as our ‘exhaustive summary’, while stochastic or simulation-based  
 533 models generally need more carefully defined data distribution parameters such as moment  
 534 dynamics equations [9]. Additionally, while our approach applies in principle to larger models,  
 535 we deliberately considered examples with low parameter dimension, as even these give complex  
 536 results. Further work could explore applications to larger models and spatially/temporally  
 537 varying parameters, as well as improving scaling and rounding heuristics for interpretable  
 538 parameter combinations.

539 The provided Julia implementation makes our methodology accessible for both analysis  
 540 and further development. We believe IIR will prove valuable for model development and  
 541 analysis across the quantitative sciences, particularly in complex applications where symbolic  
 542 approaches may be impractical.

543 **6. Acknowledgements.** Parts of this work were carried out at the MATRIX Workshop  
 544 on Parameter Identifiability in Mathematical Biology (2024) for which OJM and MJS were  
 545 among the organisers. We thank MATRIX for funding this workshop and the participants for  
 546 their stimulating discussions. MJS was supported by the Australian Research Council Centre  
 547 of Excellence for Mathematical Analysis of Cellular Systems grant no. CE230100001 (MJS).

548 **7. Author Contributions.** All authors contributed to the review and editing of the man-  
 549 uscript. OJM wrote the original draft with contributions from MJS. Both OJM and MJS  
 550 contributed to the conceptualisation of the article, choice of examples and design of numerical  
 551 experiments. OJM developed the method details, proofs, wrote the code, and performed the  
 552 numerical experiments, with discussion and input from the other authors.

553 **8. Competing interests.** The authors declare that they have no competing interests.

554 **9. Data and materials availability.** All data needed to evaluate the conclusions in the  
 555 paper are present in the paper and/or the supplementary material. Julia code associated with  
 556 this paper is available from GitHub at <https://github.com/omaclarens/reparam>.

557

## REFERENCES

- 558 [1] M. AITKIN, *Statistical inference: an integrated Bayesian/likelihood approach*, CRC Press, 2010.
- 559 [2] M. AITKIN AND M. STASINOPoulos, *Likelihood analysis of a binomial sample size problem*, Contributions  
 560 to probability and statistics: Essays in honor of Ingram Olkin, (1989), pp. 496–499.
- 561 [3] G. I. BARENBLATT, *Scaling*, Cambridge University Press, 2003.
- 562 [4] J. BEAR, *Dynamics of fluids in porous media*, American Elsevier Publishing Company, 1972.
- 563 [5] G. BELLU, M. P. SACCOMANI, S. AUDOLY, AND L. D’ANGIÓ, *Daisy: A new software tool to test global  
 564 identifiability of biological and physiological systems*, Computer Methods and Programs in Biomedicine, 88 (2007), pp. 52–61.
- 565 [6] R. BIRD, W. STEWART, AND E. LIGHTFOOT, *Transport phenomena*, no. v. 1 in Transport Phenomena,  
 566 Wiley, 2006.
- 567 [7] K. S. BROWN, C. C. HILL, G. A. CALERO, C. R. MYERS, K. H. LEE, J. P. SETHNA, AND R. A.  
 568 CERIONE, *The statistical mechanics of complex signaling networks: nerve growth factor signalling*,  
 569 Physical Biology, 1 (2004), p. 184.
- 570 [8] K. S. BROWN AND J. P. SETHNA, *Statistical mechanical approaches to models with many poorly known  
 571 parameters*, Physical Review E, 68 (2003), p. 021904.

- 573 [9] A. P. BROWNING, D. J. WARNE, K. BURRAGE, R. E. BAKER, AND M. J. SIMPSON, *Identifiability*  
574 *analysis for stochastic differential equation models in systems biology*, Journal of the Royal Society  
575 Interface, 17 (2020), p. 20200652.
- 576 [10] E. BUCKINGHAM, *On physically similar systems; illustrations of the use of dimensional equations*, Physical  
577 review, 4 (1914), p. 345.
- 578 [11] H. CARS LAW AND J. JAEGER, *Conduction of heat in solids*, Oxford science publications, Clarendon Press,  
579 1959.
- 580 [12] E. A. CATCHPOLE AND B. J. MORGAN, *Detecting parameter redundancy*, Biometrika, 84 (1997), pp. 187–  
581 196.
- 582 [13] E. A. CATCHPOLE, B. J. T. MORGAN, AND S. N. FREEMAN, *Estimation in parameter-redundant models*,  
583 Biometrika, 85 (1998), pp. 462–468.
- 584 [14] M. J. CHAPPELL AND R. N. GUNN, *A procedure for generating locally identifiable reparameterisations*  
585 *of unidentifiable non-linear systems by the similarity transform approach*, Mathematical Biosciences,  
586 148 (1998), pp. 21–41.
- 587 [15] O. CHIŞ, J. R. BANGA, AND E. Balsa-CANTO, *Structural identifiability of systems biology models: a*  
588 *critical comparison of methods*, Plos One, 6 (2011), p. e27755.
- 589 [16] O. CHIŞ, A. F. VILLAVERDE, J. R. BANGA, AND E. Balsa-CANTO, *On the relationship between sloppiness*  
590 *and identifiability*, Mathematical Biosciences, 282 (2016), pp. 147–161.
- 591 [17] D. COLE, *Parameter redundancy and identifiability*, CRC Press, 2020.
- 592 [18] D. J. COLE, B. J. T. MORGAN, AND D. M. TITTERINGTON, *Determining the parameteric structure of*  
593 *models*, Mathematical Biosciences, 228 (2010), pp. 16–30.
- 594 [19] P. G. CONSTANTINE, C. KENT, AND T. BUI-THANH, *Accelerating markov chain monte carlo with active*  
595 *subspaces*, SIAM Journal on Scientific Computing, 38 (2016), pp. A2779–A2805.
- 596 [20] D. R. COX, *Principles of statistical intererence*, Cambridge University Press, 2006.
- 597 [21] D. R. COX AND N. REID, *Parameter orthogonality and approximate conditional inference*, Journal of the  
598 Royal Statistical Society: Series B (Methodological), 49 (1987), pp. 1–18.
- 599 [22] J. CRANK, *The mathematics of diffusion*, Oxford university press, 1979.
- 600 [23] T. CUI, J. MARTIN, Y. M. MARZOUK, A. SOLONEN, AND A. SPANTINI, *Likelihood-informed dimension*  
601 *reduction for nonlinear inverse problems*, Inverse Problems, 30 (2014), p. 1100998.
- 602 [24] T. CUI AND X. TONG, *A unified performance analysis of likelihood-informed subspace methods*, Bernoulli,  
603 28 (2022), pp. 2788–2815.
- 604 [25] S. DÍAZ-SEOANE, X. REY BARREIRO, AND A. F. VILLAVERDE, *STRIKE-GOLDD 4.0: User-friendly,*  
605 *efficient analysis of structural identifiability and observability*, Bioinformatics, 39 (2022), p. btac748.
- 606 [26] C. R. ELEVITCH AND C. R. JOHNSON JR, *A procedure for ranking parameter importance for estimation*  
607 *in predictive mechanistic models*, Ecological Modelling, 419 (2020), p. 108948.
- 608 [27] N. D. EVANS AND M. J. CHAPPELL, *Extensions to a procedure for generating locally identifiable repa-*  
609 *rameterisations of unidentifiable systems*, Mathematical Biosciences, 168 (2000), pp. 137–159.
- 610 [28] C. R. FITTS, *Groundwater science*, Elsevier, 2002.
- 611 [29] A. GELMAN, *Parameterization and bayesian modeling*, Journal of the American Statistical Association,  
612 99 (2004), pp. 537–545.
- 613 [30] A. GRIEWANK AND A. WALTHER, *Evaluating derivatives: principles and techniques of algorithmic differ-*  
614 *entiation*, SIAM, 2008.
- 615 [31] R. N. GUTENKUNST, J. J. WATERFALL, F. P. CASEY, K. S. BROWN, C. R. MYERS, AND J. P. SETHNA,  
616 *Universally sloppy parameter sensitivities in systems biology models*, PLOS Computational Biology,  
617 3 (2007), p. e189.
- 618 [32] D. F. HENDRY AND M. S. MORGAN, *The foundations of econometric analysis*, Cambridge University  
619 Press, 1997.
- 620 [33] K. E. HINES, T. R. MIDDENDORF, AND R. W. ALDRICH, *Determination of parameter identifiability*  
621 *in nonlinear biophysical models: A Bayesian approach*, Journal of General Physiology, 143 (2014),  
622 p. 401.
- 623 [34] A. HOLMBERG, *On the practical identifiability of microbial growth models incorporating michaelis-menten*  
624 *type nonlinearities*, Mathematical Biosciences, 62 (1982), pp. 23–43.
- 625 [35] F. HORN AND R. JACKSON, *General mass action kinetics*, Archive for Rational Mechanics and Analysis,  
626 47 (1972), pp. 81–116.

- 627 [36] P. HOWELL, G. KOZYREFF, AND J. OCKENDON, *Applied Solid Mechanics*, Cambridge University Press,  
628 2008.
- 629 [37] K. A. JOHNSON AND R. S. GOODY, *The original michaelis constant: Translation of the 1913  
630 michaelis–menten paper*, Biochemistry, 50 (2011), pp. 8264–8269.
- 631 [38] M. KOT, *Elements of Mathematical Ecology*, Cambridge University Press, 2001.
- 632 [39] W. B. KRANTZ, *Scaling Analysis in Modeling Transport and Reaction Processes*, Wiley Interscience, 2007.
- 633 [40] C. KREUTZ, A. RAUE, D. KASCHEK, AND J. TIMMER, *Profile likelihood in systems biology*, The FEBS  
634 Journal, 280 (2013), pp. 2564–2571.
- 635 [41] C. KREUTZ, A. RAUE, AND J. TIMMER, *Likelihood-based observability analysis and confidence intervals  
636 for predictions of dynamics models*, BMC Systems Biology, 6 (2012).
- 637 [42] J. LAWRIE AND J. HEARNE, *Reducing model complexity via output sensitivity*, Ecological Modelling, 207  
638 (2007), pp. 137–144.
- 639 [43] F. W. LAWVERE AND R. ROSEBRUGH, *Sets for mathematics*, Cambridge University Press, 2003.
- 640 [44] J. LEE, *Introduction to smooth manifolds*, Graduate Texts in Mathematics, Springer New York, 2013.
- 641 [45] T. S. LIGON, F. FRÖLICH, O. CHİŞ, J. R. BANGA, E. Balsa-Canto, AND J. HASENAUER, *Gensis  
642 2.0: multi-experimental structural identifiability analysis of sbml models*, Bioinformatics, 34 (2018),  
643 pp. 1421–1423.
- 644 [46] O. J. MACLAREN AND R. NICHOLSON, *What can be estimated? identifiability, estimability, causal inference  
645 and ill-posed inverse problems*, arxiv preprint, 1904.02826 (2019).
- 646 [47] O. J. MACLAREN AND R. NICHOLSON, *Models, identifiability, and estimability in causal inference*, in  
647 Workshop on the Neglected Assumptions in Causal Inference (NACI) at the 38th International Conference  
648 on Machine Learning, 2021, 2021.
- 649 [48] J. R. MAGNUS AND H. NEUDECKER, *Matrix differential calculus with applications in statistics and econo-  
650 metrics*, John Wiley & Sons, 2019.
- 651 [49] T. MAIWALD, H. HASS, B. STEIERT, J. VANLIER, R. ENGESSER, A. RAUE, F. KIPKEEW, H. H. BOCK,  
652 D. KASCHEK, C. KREUTZ, AND J. TIMMER, *Driving the model to its limit: Profile likelihood based  
653 model reduction*, Plos One, 11 (2016), p. e0162366.
- 654 [50] N. MESHKAT, M. EISENBERG, AND J. J. DiSTEFANO III, *An algorithm for finding globally identifiable  
655 parameter combinations of nonlinear ode models using Gröbner bases*, Mathematical Biosciences, 222  
656 (2009), pp. 61–72.
- 657 [51] N. MESHKAT, S. SULLIVANT, AND M. EISENBERG, *Identifiability results for several classes of linear  
658 compartment models*, Bulletin of Mathematical Biology, 77 (2015), p. 1620–1651.
- 659 [52] J. MONOD, *The growth of bacterial cultures*, Annual Review of Microbiology, 3 (1949), pp. 371–394.
- 660 [53] G. M. MONSALVE-BRAVO, B. A. J. LAWSON, C. DROVANDI, K. BURRAGE, K. S. BROWN, C. M.  
661 BAKER, S. A. VOLLERT, K. MENGERSEN, E. McDONALD-MADDEN, AND M. P. ADAMS, *Analysis  
662 of sloppiness in model simulations: Unveiling parameter uncertainty when mathematical models are  
663 fitted to data*, Science Advances, 8.
- 664 [54] G. M. MONSALVE-BRAVO, B. A. J. LAWSON, C. DROVANDI, K. BURRAGE, K. S. BROWN, C. M.  
665 BAKER, S. A. VOLLERT, K. MENGERSEN, E. McDONALD-MADDEN, AND M. P. ADAMS, *Analysis  
666 of sloppiness in model simulations: unveiling parameter uncertainty when mathematical models are  
667 fitted to data*, Science Advances, 8 (2022), p. eabm5952.
- 668 [55] R. J. MURPHY, O. J. MACLAREN, AND M. J. SIMPSON, *Implementing measurement error models with  
669 mechanistic mathematical models in a likelihood-based framework for estimation, identifiability analy-  
670 sis and prediction in the life sciences*, Journal of the Royal Society Interface, 21 (2024), p. 20230402.
- 671 [56] J. MURRAY, *Mathematical biology I: An introduction*, Springer, 2002.
- 672 [57] I. OLKIN, A. J. PETKAU, AND J. V. ZIDEK, *A comparison of n estimators for the binomial distribution*,  
673 Journal of the American Statistical Association, 76 (1981), pp. 637–642.
- 674 [58] L. PACE AND A. SALVAN, *Principles of statistical inference from a neo-Fisherian perspective*, World  
675 Scientific, 1997.
- 676 [59] Y. PAWITAN, *In all likelihood: statistical modelling and inference using likelihood*, Oxford University Press,  
677 2001.
- 678 [60] A. RAUE, J. KARLSSON, M. P. SACCOMANI, M. JIRSTRAND, AND J. TIMMER, *Structural and practi-  
679 cal identifiability analysis of partially observed dynamical models by exploiting the profile likelihood*,  
680 Bioinformatics, 30 (2014), pp. 1440–1448.

- 681 [61] J. REVELS, M. LUBIN, AND T. PAPAMARKOU, *Forward-mode automatic differentiation in Julia*, arXiv  
682 preprint arXiv:1607.07892, (2016).
- 683 [62] K. R. RUSHTON, *Groundwater hydrology: conceptual and computational models*, John Wiley & Sons,  
684 2004.
- 685 [63] M. J. SIMPSON, R. E. BAKER, S. T. VITTADELLO, AND O. J. MACLAREN, *Parameter identifiability  
686 analysis for spatiotemporal models of cell invasion*, Journal of the Royal Society Interface, 17 (2020).
- 687 [64] M. J. SIMPSON AND O. J. MACLAREN, *Profile-wise analysis: A profile likelihood-based workflow for iden-  
688 tifiability analysis, estimation, and prediction with mechanistic mathematical models*, PLOS Compu-  
689 tational Biology, 19 (2023), p. e1011515.
- 690 [65] M. J. SIMPSON AND O. J. MACLAREN, *Making predictions from nonidentifiable models.*, Bulletin of  
691 Mathematical Biology, 86 (2024), p. 80.
- 692 [66] G. STEWART, *Matrix perturbation theory*, Computer Science and Scientific Computing/Academic Press,  
693 Inc, (1990).
- 694 [67] J. TRENT, *Likelihood-based computational analysis and uncertainty quantification for mechanistic models*,  
695 master's thesis, University of Auckland, 2024.
- 696 [68] A. F. VILLAVERDE, E. RAIMÚNDEZ, J. HASENAUER, AND J. R. BANGA, *Assessment of prediction uncer-  
697 tainty quantification methods in systems biology*, IEEE/ACM Transactions on Computational Biology  
698 and Bioinformatics, 30 (2023), pp. 1725–1736.
- 699 [69] S. A. VOLLETT, C. DROVANDI, G. M. MONSALVE-BRAVO, AND M. P. ADAMS, *Strategic model reduc-  
700 tion by analysing model sloppiness: A case study in coral calcification*, Environmental Modelling &  
701 Software, 159 (2023), p. 105578.
- 702 [70] F.-G. WIELAND, A. L. HAUBER, M. ROSENBLATT, T. C, AND J. TIMMER, *On structural and practical  
703 identifiability.*, Current Opinion in Systems Biology, 25 (2021).